Mode Mixity and Constraint Parameters Accounting for Crack Tip Curvature

V.N.Shlyannikov[1,a], S.Yu.Kislova[1,b]

[1] Lobachevsky Street, 2/31, post-box 190, Kazan, 420111, Russia
[a] shlyannikov@mail.ru, [b] svetlana_kislova@mail.ru

Keywords: mixity and constraint parameters, crack growth angle, finite element analysis, small scale yielding, second order stress field, elastic-plastic behavior of the material, radial and angular stress distributions.

Abstract. The results of calculations for both elastic-plastic mixity and constraint parameters in full range of mode I and mode II combinations accounting for crack-tip curvature are presented. Full-field finite element analysis based on a modified boundary layer approach is employed to model the mode mixity effects on elastic-plastic crack tip behavior. The present work is based on the assumption that the tangential stresses have to have extremum along the crack growth direction. The elastic-plastic mode mixity parameter has been found accounting for the crack tip curvature. The mode mixity parameter has been obtained as ratio of tangential full stress to shear full stress ahead of crack tip. From this point of view, nonlinear analysis has been made by solving the partial differential equations governing the dominant singularity to study the displacements, stresses and strains near the crack tip for the complete range of mixed mode loading between Mode I and II. To determine the constraint parameter an additive decomposition is used for the actual full-field stress at the crack tip into a reference field and second order stress field. For the reference field the HRR-type analytical solutions have been used as well as the corresponding full range of in-plane mixed mode small scale yielding conditions. It is found that the constraint factor under mixed mode loading is strongly dependent upon the crack tip curvature. The relations between a constraint factor of the second-order stress field and mode mixity parameter for different crack tip curvature values are determined.

Introduction

Several analytical and numerical studies have been undertaken to analyze stress-strain state at the tip in order understand elastic-plastic mixed-mode crack behavior. Authors [1,2] have examined the line crack subjected to combined Mode I and Mode II loading using a small scale yielding analysis of an elastic-plastic body under plane strain conditions (i.e. extending the HRR-type solution on Mode I fracture to the mixed mode case). The analysis was only related to the mathematically edgy crack and the first term of near-tip asymptotic stress expansion. Moreover, only limited studies were conducted in the past to study the effect of higher order terms on the initiation of mixed mode fracture under predominantly elastic-plastic stress strain state. Although there has been a wide range of studies on the effects of constraint for mode I, at the same time very little research has been reported in the literature for general mixed mode conditions. Most of the above analyses on the constraint effect focused on the determination of second order term amplitude and stress angular distributions under mode I conditions [3-5]. A similar constraint effect investigation for inclined cracks in elastic-plastic solids accounting for crack tip curvature has not been carried out in the past.

The main objective of the present work is to study the effect of the crack tip constraint for general mixed mode loading with taking into account a crack tip curvature. Our investigation is carried out within the framework of elastic-plastic mixed-mode (combining Mode I and Mode II) plane strain conditions.

The modified boundary layer approach

The geometry considered in this work is traditional for the modified boundary layer formulation. A biaxially loaded cracked panel (Fig.1) is imagined which contains an annular region where the local stress field under arbitrary remote loading may be essentially characterized by a scaleable eigensolution

$$\begin{aligned}
\sigma_{xx} &= \frac{K_1}{\sqrt{2\pi r}}\left[cos\frac{\theta}{2}\left(1-sin\frac{\theta}{2}sin\frac{3\theta}{2}\right)-\frac{\rho}{2r}cos\frac{3\theta}{2}\right]-\frac{K_2}{\sqrt{2\pi r}}\left[sin\frac{\theta}{2}\left(2+cos\frac{\theta}{2}cos\frac{3\theta}{2}\right)-\frac{\rho}{2r}sin\frac{3\theta}{2}\right]+T\\
\sigma_{yy} &= \frac{K_1}{\sqrt{2\pi r}}\left[\cos\frac{\theta}{2}\left(1+\sin\frac{\theta}{2}\sin\frac{\theta}{2}\right)+\frac{\rho}{2r}\cos\frac{3\theta}{2}\right]+\frac{K_2}{\sqrt{2\pi r}}\left(\sin\frac{\theta}{2}\cos\frac{\theta}{2}\cos\frac{3\theta}{2}-\frac{\rho}{2r}\sin\frac{3\theta}{2}\right)\qquad(1)\\
\sigma_{xy} &= \frac{K_1}{\sqrt{2\pi r}}\left(\sin\frac{\theta}{2}\cos\frac{\theta}{2}\cos\frac{3\theta}{2}-\frac{\rho}{2r}\sin\frac{3\theta}{2}\right)+\frac{K_2}{\sqrt{2\pi r}}\left[\cos\frac{\theta}{2}\left(1-\sin\frac{\theta}{2}\sin\frac{3\theta}{2}\right)-\frac{\rho}{2r}\cos\frac{3\theta}{2}\right],
\end{aligned}$$

$$T=\sigma(1-\eta)\cos 2\beta \qquad (2)$$

Here T is the non-singular second order term or the T-stress, σ is the nominal stress applied in the Y-axis direction, β is the inclined crack angle referred to the Y-axis, η is the biaxial stress ratio, r and θ are polar coordinates centered at the crack tip.

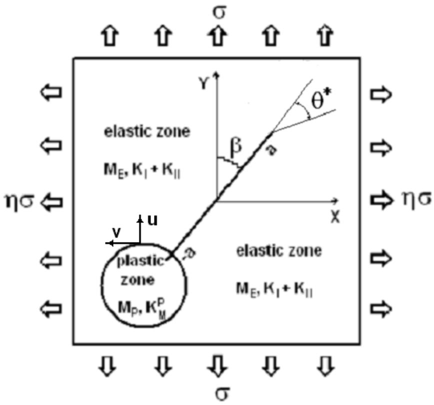

Fig. 1. The biaxially loaded inclined crack and the direction θ^* of crack propagation.

Different degrees of biaxiality and mixed mode are given by the combinations of β and η. Tensile load corresponds to $\beta=90^\circ$ for any η, and pure shear load to $\beta=45^\circ$, $\eta=-1$. The displacement components based on the first two terms of the elastic crack tip field which are given by [6]

$$\left\{\begin{aligned}
u &= \frac{K_1}{G}\sqrt{\frac{r}{2\pi}}cos\frac{\theta}{2}\left[\frac{1}{2}(\kappa-1)+sin^2\frac{\theta}{2}\right]+\frac{K_2}{G}\sqrt{\frac{r}{2\pi}}sin\frac{\theta}{2}\left[\frac{1}{2}(\kappa+1)+cos^2\frac{\theta}{2}\right]+\\
&+\frac{(1-\eta)\sigma}{8G}\{r[cos(\theta+2\beta)+\kappa\, cos(\theta-2\beta)-2\,sin\,\theta\,sin\,2\beta]+(\kappa+1)a\,cos\,2\beta\}\\
v &= \frac{K_1}{G}\sqrt{\frac{r}{2\pi}}sin\frac{\theta}{2}\left[\frac{1}{2}(\kappa+1)-cos^2\frac{\theta}{2}\right]+\frac{K_2}{G}\sqrt{\frac{r}{2\pi}}cos\frac{\theta}{2}\left[\frac{1}{2}(1-\kappa)+sin^2\frac{\theta}{2}\right]+\\
&+\frac{(1-\eta)\sigma}{8G}\{r[sin(2\beta-\theta)+\kappa\, sin(2\beta+\theta)-2\,sin\,\theta\,cos\,2\beta]+(\kappa+1)a\,sin\,2\beta\}
\end{aligned}\right. \qquad (3)$$

$$K_1 = \frac{\sigma\sqrt{\pi a}}{2}\left[(1+\eta)-(1-\eta)\cos 2\beta\right]; \quad K_2 = \frac{\sigma\sqrt{\pi a}}{2}\left[(1-\eta)\sin 2\beta\right] \tag{4}$$

are prescribed on the outer boundary of the domain. In above equations, K_I and K_2 are the mode I and II stress intensity factors, respectively. Further, G and a are the shear modulus and the crack length, and $\kappa = 3-4\nu$ where ν is the Poisson's ratio. A circular disc containing the crack tip in a large panel is removed, modeling the near tip region with the modified boundary layer formulation. These elastic displacements corresponding to the different mixed mode state were applied along the circular boundary of the R radius (Fig.1).

The biaxial loads are applied through the stress intensity factors and the transverse T-stress. The panel was subjected to biaxial loading with a large number of the initial crack angle β. Varied values of β at η= -1 and resulting T-stress and both elastic and plastic mode mixity parameters with crack growth direction angle θ^* are listed in Table 1 for the mathematical notch (ρ=0), where $\bar{T} = T/\sigma_0$ is normalized by the yield stress σ_0.

Table 1. Values of varied parameters in numerical calculations

β [°]	45	50	55	60	65	70	75	80	85	90
$\bar{T}$	0.00	-0.138	-0.272	-0.397	-0.511	-0.609	-0.688	-0.747	-0.783	-0.795
$M_e\vert_{\rho=0}$	0.00	0.111	0.222	0.333	0.444	0.556	0.667	0.778	0.889	1.00
$M_p\vert_{\rho=0}$	0.00	0.165	0.337	0.461	0.581	0.688	0.772	0.852	0.909	1.00
$\theta^*\vert_{\rho=0}$	-75.0	-69.6	-64.3	-59.7	-53.8	-46.7	-38.6	-27.5	-18.2	0.00

Mode mixity parameters determination

For an elastic and isotropic plate, under conditions of plane strain, containing a slant internal crack of length $2a$ and obliqueness β, which is submitted at infinity to a biaxial state of stress, the elastic mode mixity parameter M_E of stresses at the crack tip with mathematical notch ($\rho = 0$) takes the form as follows

$$M_E = \frac{2}{\pi}\tan^{-1}\left|\lim_{r\to\infty}\frac{\sigma_{\theta\theta}(\theta=0)}{\sigma_{r\theta}(\theta=0)}\right| = \frac{2}{\pi}\tan^{-1}\left|\frac{K_I}{K_{II}}\right| = \frac{2}{\pi}\tan^{-1}\left|\frac{(1+\eta)-(1-\eta)\cos 2\beta}{(1-\eta)\sin 2\beta}\right|. \tag{5}$$

For the case of the crack with finite tip curvature radius, the elastic crack-field mode mixity parameter M_E^* expressed by relation (1) and (2), is given by

$$M_E^* = \frac{2}{\pi}\tan^{-1}\left|\frac{K_I[2r+\rho]}{K_{II}[2r-\rho]}\right| = \frac{2}{\pi}\tan^{-1}\left|\frac{[(1+\eta)-(1-\eta)cos\,2\beta](2r+\rho)}{[(1-\eta)sin\,2\beta](2r-\rho)}\right|. \tag{6}$$

For the mixed mode small scale yielding problem, the near-field mixity parameter M_p introduced by Shih [1] is required to specify the stress and strain fields in the vicinity of the mathematically edgy crack tip ($\rho = 0$) in the following form

$$M_p = \frac{2}{\pi}\tan^{-1}\left|\frac{\tilde{\sigma}_{\theta\theta}(\theta=0)}{\tilde{\sigma}_{r\theta}(\theta=0)}\right| \tag{7}$$

As follows from the Shlyannikov's plastic mixed mode solution [2] based on the new method for boundary conditions, the angular distribution of stresses and strains depends on the crack growth direction angle θ^*. Based on the new scheme of mixed mode problem solution the mixity parameters M_E, M_P, I_n and relation between M_E and M_P are given as function of the crack growth direction criterion and the strain hardening exponent. From these solutions for each particular value of $\theta^* = \theta^*(\sigma, \beta, \eta, \nu, r/a)$ the angular dimensionless stress components $\tilde{\sigma}_{\theta\theta}$ and $\tilde{\sigma}_{r\theta}$ distributions ranging from pure Mode I to pure Mode II are found. Thus, the crack deviation angle θ^* to identify each possible set of dimensionless stresses and strains fields under mixed mode loading. Unlike the investigation of Shih [1], the plastic mixity parameter M_p for the mathematically edgy crack in the present work was directly obtained from both dimensionless $\tilde{\sigma}_{\theta\theta}$ and $\tilde{\sigma}_{r\theta}$ distributions without an analysis of intermediate fields.

In the case of elastic-plastic mixed mode problem for inclined crack with finite crack-tip curvature the numerical computation on the base of FEM is used to obtain nonlinear stress-strain state under biaxial loading. The mode mixity parameter M_P^* in this case has been obtained as ratio of tangential full stress to shear full stress ahead of crack tip

$$M_P^* = \frac{2}{\pi} \tan^{-1} \left| \frac{\bar{\sigma}_{\theta\theta}^{FEM}(\rho, r, \theta = 0)}{\bar{\sigma}_{r\theta}^{FEM}(\rho, r, \theta = 0)} \right| \tag{8}$$

Note that the crack growth direction angle $\theta^* = \theta^*(\sigma, \beta, \eta, \nu, r/a)$ is a function of mode mixity and biaxiality parameters expressed in the form of a fracture criterion. Several different criteria have been proposed for determining the direction of crack growth under general mixed mode loading conditions. The present study deals with an application of the maximum tangential stress criterion, because it is corresponding to dominant fracture mechanism. The crack is considered to extend in the radial direction for which the basis function has an extremum, and the propagation begins when the function reaches a critical value. In the case of the maximum tangential stress criterion by Erdogan and Sih [7], the crack is considered to extend from the crack tip in the radial direction θ^* given by the point of maximum tangential stress $\sigma_{\theta\theta}$ on a circle of finite radius from the point of fracture initiation. The crack propagation angle θ^* is measured negative clockwise from the crack axis and passing through the point of fracture initiation.

Constraint parameter determination

It is apparent from the literature that the asymptotic analyses based on a higher-order terms power expansion did not provide the solution for angular stress distribution concerning to mixed mode loading. Therefore in the present work the full field numerical solution $\bar{\sigma}_{ij}^{FEM}(r,\theta)$ to the two parameters boundary layer formulation is taken to be the exact solution. A two-term generalized asymptotic expansion of the stress function was used to describe the stress field in the vicinity of the inclined crack tip with finite curvature radius in a power hardening material in the following form

$$\bar{\sigma}_{ij}^{FEM}(r,\theta) = \frac{\sigma_{ij}^{FEM}(r,\theta)}{\sigma_0} = \bar{\sigma}_{ij}^{REF}(\bar{r}, \theta, n, M_P) + Q + \ldots \tag{9}$$

where

$$\bar{\sigma}_{ij}^{REF}(\bar{r}, \theta, n, M_P) = (\bar{\alpha} I_n \bar{r})^{-1/(n+1)} \tilde{\sigma}_{ij}^{REF}(\theta, n, M_P), \tag{10}$$

$$Q = A\bar{r}^{\lambda}\tilde{\sigma}_{ij}^{(1)}\left(\theta, n, M_P^*\right), \tag{11}$$

$$\bar{r} = \left(\sigma_0 r/J\right),\ J = \sqrt{J_1^2 + J_2^2}\ ,\ J_1 = \frac{(1+\nu)(1+\kappa)}{4E}\left(K_1^2 + K_2^2\right),\ J_2 = -\frac{(1+\nu)(1+\kappa)}{2E}K_1 K_2 .$$

Here ε_0 is yield strain, $\bar{\alpha} = \alpha\varepsilon_0$ and I_n is an integration constant, which is a function polar angle θ, hardening exponent n and mode mixity M_P. The first term of Eq. (9) represents the reference mixed mode solution for the mathematically edgy crack, where dimensionless angular functions $\tilde{\sigma}_{ij}^{REF}\left(\theta, n, M_P\right)$ have been determined by solution of the nonlinear fourth-order differential compatibility strain equation and given by Shlyannikov [2]. The second term or the Q-stress in the expansion (9) is supposed to characterize effects of in-plane constraint under elastic-plastic mixed mode fracture. The second crack tip field parameter (11) is obtained as the difference parameter between the full stress field and the reference solution (10).

Resolving Equation (9) relatively $\tilde{\sigma}_{ij}^{(1)}\left(\theta, n, M_P^*\right)$ the second order term angular variation can be easily obtained as the difference field between the normalized full stress field and the reference stress field

$$\tilde{\sigma}_{ij}^{(1)}\left(\theta, n, M_P^*\right) = \left[\bar{\sigma}_{ij}^{FEM}\left(r, \theta\right) - \bar{\sigma}_{ij}^{REF}\left(\theta, n, M_P\right)\right] / A\bar{r}^{\lambda} \tag{12}$$

In this equation the value of $A\bar{r}^{\lambda}$ plays the role of a scale factor which normalizes the effective stress $\tilde{\sigma}_{e}^{(1)}\left(\theta, n, M_P^*\right)$ so that $\left(3\tilde{s}_{ij}^{(1)}\tilde{s}_{ij}^{(1)}/2\right)^{1/2} = 1$ (where $\tilde{s}_{ij}$ is the deviatoric stress tensor).

It is necessary to remind that method [2] enable to directly connect the near-field to the far-field throughout the fracture initiation angle θ^*. The satisfaction of the crack propagation criterion at $\theta=\theta^*$ implies that in this direction the maximum of the tangential stress $\bar{\sigma}_{\theta\theta}$ will take place at some distance from the crack tip. Consequently, our approach makes it possible to obtain the second order term exponent λ considering two crack-tip distances $\bar{r}_1$ and $\bar{r}_2$ where the boundary conditions so that the tangential stress $\sigma_{\theta\theta}$ has extrema along the crack growth direction $\theta = \theta^*$ are satisfied

$$\lambda = \frac{ln\left\{\left[\left(\bar{\sigma}_{\theta\theta}^{FEM}\left(\bar{r}_2, \theta^*\right) - \bar{\sigma}_{\theta\theta}^{REF}\left(\bar{r}_2, \theta^*\right)\right) / \tilde{\sigma}_{\theta\theta}^{(1)}\left(\bar{r}_2, \theta^*\right)\right] / \left[\left(\bar{\sigma}_{\theta\theta}^{FEM}\left(\bar{r}_1, \theta^*\right) - \bar{\sigma}_{\theta\theta}^{REF}\left(\bar{r}_1, \theta^*\right)\right) / \tilde{\sigma}_{\theta\theta}^{(1)}\left(\bar{r}_1, \theta^*\right)\right]\right\}}{ln\left(\bar{r}_2/\bar{r}_1\right)} . \tag{13}$$

Substituting $\tilde{\sigma}_{\theta\theta}^{(1)}\left(\theta^*, n, M_P^*\right)$ from Equation (12) and taking both the reference solution for angular distribution of $\tilde{\sigma}_{\theta\theta}^{REF}\left(\theta^*, n, M_P\right)$ and the second order term exponent λ for corresponding case of mixed mode loading one has the following final expression for the second order stress amplitude

$$A = \bar{r}_1^{-\lambda}\left[\bar{\sigma}_{\theta\theta}^{FEM}\left(\bar{r}_1, \theta^*\right) - \bar{\sigma}_{\theta\theta}^{REF}\left(\bar{r}_1, \theta^*\right)\right] / \tilde{\sigma}_{\theta\theta}^{(1)}\left(\bar{r}_1, \theta^*\right) \tag{14}$$

In order to study the various interdependences of biaxial load configuration and constrain parameters, systematic finite element analyses under different mode mixity conditions are necessary, especially for the cases containing contribution of crack tip curvature.

Results and discussion

The ANSYS (1999) finite element code is used to solve modified boundary layer problems. The Ramberg-Osgood model was employed to define the stress-strain curve corresponding to the elastic-plastic material properties. For the present problem, the Young's modulus, Poisson's ratio and the yield stress were considered to be 205 GPa, 0.3 and 380 MPa. The strain hardening exponent n was 5 and $\overline{\alpha} = 3$. The state of mixity in our calculations is given by initial crack angle α variation at load biaxiality $\eta = -1$ as it is shown in Table 1. The elastic-plastic stress components near the crack tip were obtained in the present work to explore the influence of the crack tip curvature ρ/a on constraint effect under mixed mode conditions.

According to our analytical and numerical results, the radial distributions along initial crack plane at $\theta = 0$ of the elastic M_E^* and plastic M_P^* mode mixity parameters by Eqs.(6) and (8) accounting for crack-tip curvature are shown in Fig.2 for the complete range of the mixed mode loading. It is interesting to point out in Fig.2 that for all considered mixed mode cases on a crack tip contour ($r\sigma_0/J = 0$) the plastic mode mixity parameter is $M_P^* \approx 1$. It can be seen that finite strain effects related to crack tip curvature dominate for the normalized radial distance $r\sigma_0/J < 2$, while mode mixity conditions can be significant at large distances.

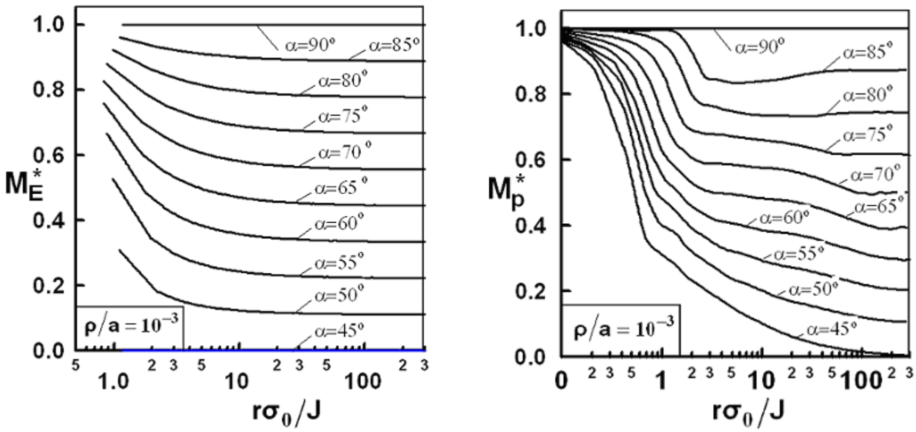

Fig. 2. Radial mode mixity parameter distributions ahead of the crack plane at θ =0°

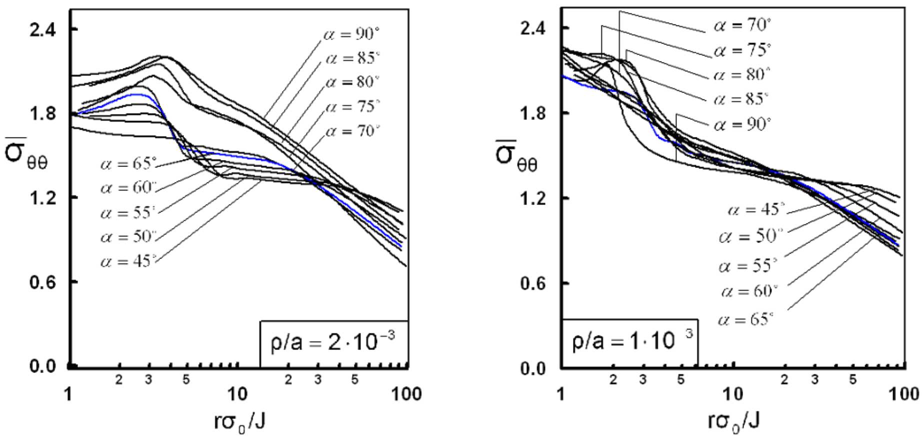

Fig. 3. Radial stress distributions in the crack growth direction at θ =θ*

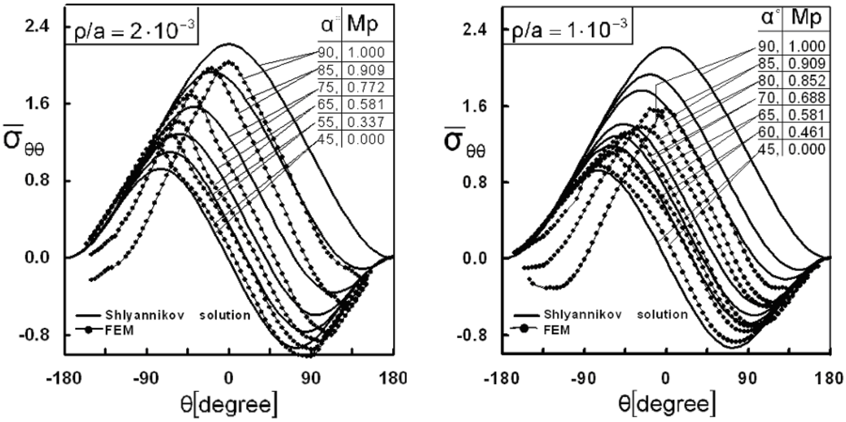

Fig. 4. Angular tangential stress distributions for different near-tip mixities

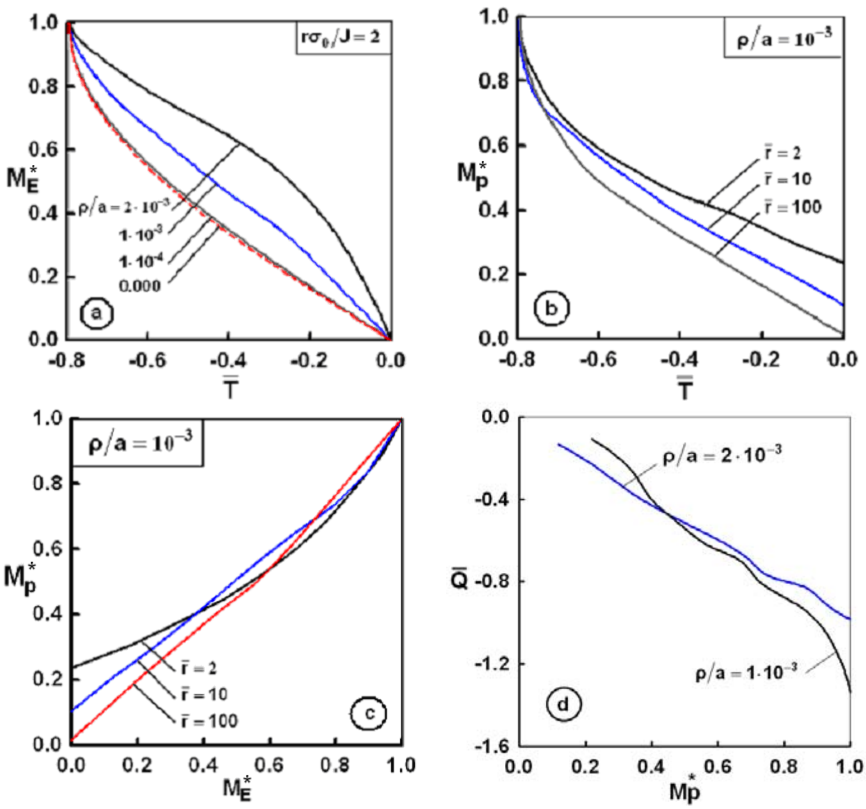

Fig. 5. Mode mixity and constraint parameters behavior accounting for crack tip curvature

Tangential stress distributions in crack growth direction ($\theta = \theta^{*}$) under mixed mode loading obtained from the full field finite element analysis are represented in Fig.3 for different dimensionless crack tip curvature values where the radial distance r is normalized by J/σ_0 . The results show that $\bar{\sigma}_{\theta\theta}(\theta=\theta^*)$ has extrema at some distances from the crack tip. The tangential stress distributions have a different tendency to change. In contrast to the $\rho/a=2\cdot10^{-3}$ case, the tangential stress $\bar{\sigma}_{\theta\theta}$ distributions at $\rho/a=1\cdot10^{-3}$ at various mode mixity values vary slightly. The radial stress $\bar{\sigma}_{\theta\theta}$ distributions for $\rho/a=2\cdot10^{-3}$ along $\theta=\theta^*$ shown in Fig.3 are more sensitive to the loading conditions.

In order to demonstrate the angular distributions of a tangential stress field for the complete range of mixed mode loading, the full field finite element results and reference fields are reported and compared in Fig.4. The full field finite element solution indicated by the symbols while the reference field indicated by solid line. These figures show the angular variations of stress fields at radial distance $r\sigma_0/J=2\div4$. It is observed that for different crack tip curvature ρ/a in Fig.4 the full field finite element solutions of the tangential stress deviate substantially from those of reference fields. This circumstance predetermines the necessity to take into account of the high order terms in the stress expansion at crack tip vicinity. Besides, when we construct the power-law solutions, we assume that the extrema of the tangential stresses $\bar{\sigma}_{\theta\theta}$ exist in the crack growth direction $\theta=\theta^*$. This fact is confirmed in Fig.4, where the angular variations of $\bar{\sigma}_{\theta\theta}$ are shown for different values of the mixity parameter M_p.

The plots in Fig.5a and 5b show the behaviour of both elastic M_E^* and plastic M_P^* mode mixity parameters as function of the non-singular term $\bar{T}$-stress at different crack tip curvature and distance values. In Fig.5c are shown dependencies between $M_P^*-M_E^*$ according to Eqs.(6) and (8) in a full range of mixed mode loadings from the pure Mode I to pure Mode II. On the base of these analytical and numerical results it is concluded that the relation of M_P^* to M_E^* depends primarily on the crack tip curvature and secondary on the crack tip distance.

The constraint factor Q defined as the difference between the finite element elastic-plastic solution and the reference field by Equation (9) is depicted for the complete range of mixed mode loading in Fig.5d for the dimensionless crack tip curvature $\rho/a=1\cdot10^{-3}$ and $\rho/a=2\cdot10^{-3}$, respectively. This figure represents the dependences between the plastic mode mixity parameter and the constraint factor. It can be seen that there are roughly linear relationship between Q and M_P^* for both considered cases. Thus, it is stated that the mixed mode loading has certain influence on the constraint factor behavior for cracks with different tip curvature.

References

[1] C.F.Shih: Fracture Analysis ASTM STP 560, American Society for Testing and Materials, Philadelphia (1974), p. 187-210.

[2] V.N.Shlyannikov: *Elastic-plastic mixed mode fracture criteria and parameters* (Springer, Berlin 2003).

[3] Y.Li and Z.Wang : Scientia Sinica (series A) 29 (1986), p. 941-955.

[4] N.P.O'Dowd and C.F.Shih: Journal of the Mechanics and Physics of Solids 39 (1991), p.989-1015.

[5] S.M.Sharma and N.Aravas: Journal of the Mechanics and Physics of Solids 39 (1991), p.1043-1072.

[6] J.Eftis and N.Subramonian: Engineering Fracture Mechanics 10 (1978), p.43-67.

[7] F.Erdogan and G.C.Sih: Trans. ASME, J. Basic Eng. 85(1963), p.519-527.